Atomic Scale Conversion of Clean Si(111):H-1×1 to Si(111)-2×1 by Electron-Stimulated Desorption

R. S. Becker, G. S. Higashi, Y. J. Chabal, and A. J. Becker
AT&T Bell Laboratories, Murray Hill, New Jersey 07974
(Received 12 July 1990)

Tunneling images of the ideal Si(111):H-1×1 surface exhibit features and electronic structure consistent with a simple termination of the surface dangling bonds by atomic hydrogen. Bombardment of the surface with low-energy (2–10 eV) electrons desorbs the hydrogen, converting the 1×1 surface phase to the 2×1 π-bonded chain. The efficiency of this process versus electron kinetic energy indicates that the desorption is mediated by promoting electrons from the σ to the σ^* band. The resultant increase in surface free energy drives a spontaneous phase transition to the 2×1. Individual 2×1 regions as small as ten surface sites have been created in this fashion.

PACS numbers: 61.16.Di, 73.20.At, 79.20.Kz

The search for an ideally terminated, nonreactive surface has been the driving force for much of the effort expended in surface science in the past 30 years. Very early on it was recognized that a simple truncation of the bulk structure was often energetically unstable, forcing many materials, especially covalently bonded semiconductors, to rearrange their surface atoms in a manner to lower this energy. Even so, these heavily reconstructed surfaces, such as Si(111)-7×7, are yet quite reactive in ambient environments. In order to minimize the role this surface reactivity plays, a number of methods have been utilized to bury or stabilize the semiconductor-vacuum interfaces. Oxidation of the surface layer is a common technique in technology,[1] while arsenic termination of the Si and Ge surfaces by epitaxy has been demonstrated to yield both high symmetry and greatly reduced surface reactivity.[2] The simple saturation of surface dangling bonds of the silicon and germanium surfaces with atomic hydrogen has been explored in a high-vacuum environment.[3] Recently, infrared spectroscopic measurements have shown that high-quality Si(111) surfaces with an ideal hydrogen termination may be produced using wet chemical methods.[4] The resulting surfaces not only have a very low defect and impurity density ($<10^{-3}$), but also are stable in air and in water, and can be introduced into ultrahigh vacuum (UHV) by means of a load-lock system.[5]

In this Letter, we report on scanning tunneling microscope (STM) observations performed under ultrahigh-vacuum conditions of the Si(111):H-1×1 surface prepared by wet chemical methods. The images show the H-terminated surface to be relatively clean, with sharp steps and terrace widths determined by the large-scale vicinality. The measured electronic features are characteristic of bulk Si. We further demonstrate that the atomic hydrogen terminating the Si(111) surface may be selectively removed at room temperature by electron bombardment from the STM tip using electrons with kinetic energies of 2–10 eV. The resultant Si surface then undergoes a spontaneous phase transition from the H-stabilized 1×1 to the clean 2×1 π-bonded chain. Measurements of the efficiency of this process as a function of electron energy suggest that the principal mechanism is one of promotion of an electron from the Si-H bonding orbital to the unoccupied antibonding orbital, leading to hydrogen desorption at room temperature. Areas as small as ten atomic sites have been converted from 1×1 to 2×1 using this method.

The UHV STM used in these experiments has been described elsewhere.[6] The vacuum chamber containing the microscope has facilities for sample characterization by low-energy electron diffraction (LEED) and Auger electron spectroscopy (AES). The samples, consisting of 0.20-in.-thick, Syton-polished Si(111) wafers (*n* type, arsenic doped, 0.007 Ω cm), are cut off at 1.25° along $\langle\bar{1}\bar{1}2\rangle$ in order to generate double-layer steps for imaging purposes. The sample is cleaned and terminated with hydrogen, producing Si(111):H-1×1, using a modified HF wet chemical method described previously.[4] Immediately upon rinsing with highly pure, deionized water, it is placed in a load lock, and transferred to the STM chamber after two hours of pumpdown (estimated load-lock pressure 3×10^{-7} Torr). At this point the Si(111) sample is brought into tunneling range of the STM, and imaging initiated.

Figure 1(a) shows a high-resolution image of the *as-prepared* Si(111):H-1×1 surface, detailing an atomic step, oriented along $\langle\bar{1}10\rangle$, along with residual contamination characteristic of these experiments. This contamination, apparent as fuzzy white balls in Fig. 1, is quite likely physisorbed molecules picked up at some stage of the sample loading process.[7] Figure 1(b) shows a detail of the 1×1 structure, with the lateral image scales indicated. Both of these images are acquired at 2.0-V bias, tunneling from the tip into unoccupied sample states at 250 pA. The rows corresponding to the 1×1 surface are just visible between the contamination in the large-scale image; the 1×1 features in the small-scale image correspond to a peak-to-peak height of 0.03 Å. Figure 1(c) shows the normalized conductivity $(dI/dV)/(I/V)$ of the tunnel junction *I-V* characteristic plotted against junction bias. These data are relatively

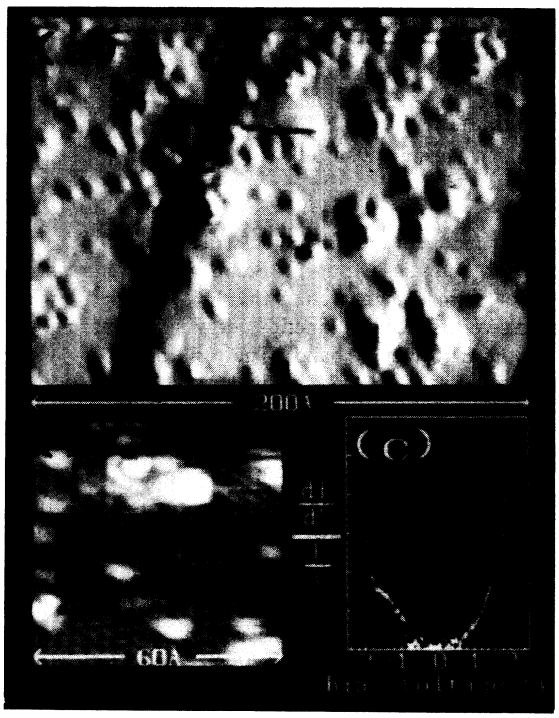

FIG. 1. (a) Tunneling image of the *as-prepared* Si(111):H-1×1 surface. (b) High-resolution image of the same showing details of the 1×1 structure. Tunneling spectrum for the 1×1 surface plotted as $(dI/dV)/(I/V)$ vs applied bias, with positive values denoting tunneling from the tip to the unoccupied sample states. The images in (a) and (b) were taken at +2.0 V at 250 pA demanded tunneling current, tunneling from the tip into empty sample states.

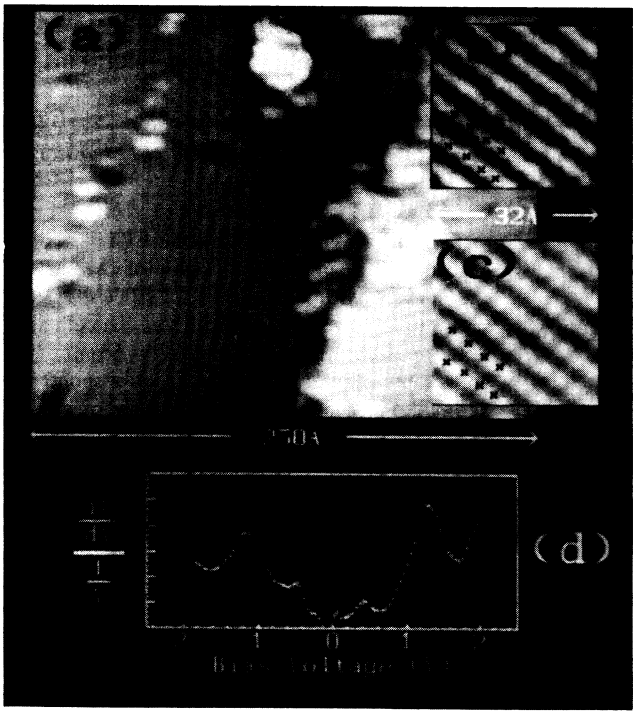

FIG. 2. (a) Tunneling images of the electron-bombarded 1×1 surface showing the resulting 2×1 domains. Simultaneous high-resolution images of one 2×1 domain depicting the phase shift along $\langle\bar{1}10\rangle$ between (b) unoccupied states and (c) occupied states. Tunneling spectrum for the 2×1 surface plotted as $(dI/dV)/(I/V)$ vs applied bias in the same manner as Fig. 1(c). The image in (a) was taken at +1.5 V at 1 nA demanded tunneling current, while the images in (b) and (c) were taken at +0.8 and −0.8 V, respectively, at 1 nA demanded tunneling current.

featureless, with an energy gap between the filled and empty tails of 1.3 eV, an occupied-state feature at −1.3 V, and a weak feature at +1.5 V. Calculations[8] predict no surface-derived states in the bulk band gap for the ideal Si(111):H surface, consistent with the spectrum shown in Fig. 1(c). Both the tunneling images and *I-V* characteristics are consistent with a model where each dangling bond of an unreconstructed Si(111) surface is saturated by one atomic hydrogen. The debris evident in both Figs. 1(a) and 1(b) occupy approximately 7% of the surface sites, with no apparent preferential adsorption sites.[7] It is remarkable that the *as-prepared* surface is sufficiently nonreactive to render the flat terraces and atomic steps the strongest features in the tunneling images, even allowing observation of the 1×1 structure with no further surface treatment.

In the natural course of our experiments on these samples, the H-terminated surface is exposed to electron bombardment during field-emission cleaning of the tunneling tip. Figure 2(a) shows tunneling images and junction *I-V* characteristics of these electron-bombarded surfaces. It is immediately apparent that the Si(111) surface has undergone a transformation from the threefold-symmetric 1×1 phase typified by Fig. 1 to a phase characterized by domains of rowlike features oriented along the principal symmetry axes of the (111) surface. Figures 2(b) and 2(c) depict a small portion of one of the domains taken at a bias of 1.0 V tunneling into unoccupied and out of occupied sample states, respectively. In Fig. 2(d), the normalized conductivity displays several strong features in the energy range −2.0–+2.0 eV. Given the symmetry and scale of these domains, it is likely that we are now imaging the 2×1 reconstruction generally found on cleaved Si(111), but occasionally detected under other conditions.[9]

The crosses in the unoccupied-state image in Fig. 2(b) denote the high points along a $\langle\bar{1}10\rangle$ row, which coincides with the low points in the simultaneous occupied-state image in Fig. 2(c). This indicates that there exists a π phase shift along $\langle\bar{1}10\rangle$ between the unoccupied and occupied surface states.[10] In Fig. 2(d), the normalized conductivity is plotted against applied bias for a rowlike domain. Strong peaks are registered at +1.2, +0.4, −0.5, and −1.2 V, in marked contrast to the analogous data shown for the H-terminated 1×1 surface in Fig. 1(c). Taken together, the data shown in Fig. 2 indicate

that the electron-bombarded surface has undergone conversion to the Si(111)-2×1 π-bonded chain structure that has been studied extensively with the STM by Feenstra and co-workers.[10,11]

While it is clear that the electron bombardment from the STM tip has instigated the conversion of the 1×1 hydrogen-terminated surface to the 2×1 π-chain surface, both the cross section and localization of the conversion reaction are requisite for determining the mechanism. For the data shown in Fig. 2, the tip is held ~1000 Å above the surface at a bias of 60–70 V; measurements with the STM indicate the resultant 2×1 region extended laterally ~8000 Å. A quick series of experiments showed that much smaller size 2×1 regions, ~40 Å in extent, could be realized by moving the tip closer to the sample and decreasing the tip bias. Since the electron energy, the beam current, and the bombarded area are all varied in these measurements, a more careful approach is required to determine the cross section.

For these cross-sectional measurements the technique of electron standing waves (ESW) is ideally suited to control the beam current and applied bias, and accurately measure the changing tip-sample distance. While the details of the technique are described elsewhere,[12] a brief description is in order: A small (~50 mV) ac signal (4 kHz) is superposed on the dc bias of the tunnel junction with lock-in techniques employed to measure the in-phase signal in the tunneling or field-emission current. This signal represents the differential conductivity (dI/dV). The dc bias is then slowly ramped up to a predetermined set point, with the STM feedback electronics maintaining constant dc current by increasing the tip-sample separation, while the dI/dV signal is recorded using a lock-in amplifier. In a single measurement we control the bombardment current and maximum applied bias, determine the tip-sample separation as a function of bias, and measure the sample work function by noting the bias condition corresponding to the first ESW peak. The bombarded surface area at any given bias will be proportional, to lowest order, to the square of the tip-sample separation, while the electron kinetic energy will be the difference between the applied bias and the measured sample work function. To determine the relative conversion efficiency, the area of the sample converted from 1×1 to 2×1 is measured from before and after tunneling images using several constant-ramp-rate end-point biases. A new area of the sample is employed for each measurement. Since this 2×1 area represents an integrated desorption measurement, the converted area is normalized by the integrated squared tip-sample separation as determined from the height versus bias data taken during the ESW measurement. This dimensionless reduced area is then plotted against end-point bias.

Figure 3 shows a series of measurements of reduced 2×1 area as a function of end-point bias. The error bars are derived from the statistics of the number of atomic sites represented by the 2×1 areas. A small amount of

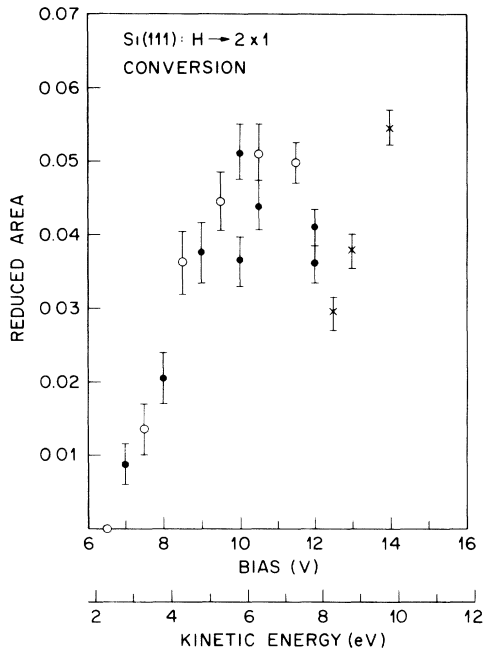

FIG. 3. Reduced 2×1 conversion area vs end-point bias for the electron-stimulated desorption of atomic hydrogen from the 1×1 surface. The different symbols indicate different data runs with the error bars derived from the statistics of the number of 2×1 sites. The lower abscissa indicates the bombarding electron's kinetic energy.

2×1 is first detected at 7-V end-point bias, increasing rapidly to a maximum at ~10 V, declining somewhat by 12 V, and then increasing rapidly. However, the abscissa here represents the difference in energy between the tip and sample Fermi levels E_F. It is more correct to consider the reduced conversion area as a function of electron kinetic energy. From the ESW data taken during the measurements plotted in Fig. 3, the sample work function ϕ is measured to be 4.17 ± 0.09 V. We note that since the samples are heavily n type, this value is reasonable as the bulk Fermi level is quite close to the bottom of the conduction band for this case. Indeed, the normalized conductivity recorded for the 2×1 π chain in Fig. 2(d) is nearly identical to that reported by Feenstra, Stroscio, and Fein[11] for n^+-doped Si(111)-2×1. The conversion efficiency in Fig. 3 is maximum at about 6 eV, with a width of ~3.5 eV. Utilizing the total electron dose, we calculate an average conversion efficiency of 3×10^{-8} for the data in Fig. 3.

The conversion-efficiency data may be compared with theoretical slab calculations by Schluter and Cohen[13] of the position of bonding and antibonding bands for various terminations of the Si(111) surface. These calculations show a Si-H σ band about 5 eV below E_F at the M and K points, bending upward and broadening as Γ is approached at an estimated 3 eV below E_F. At all points this band is resonant with the bulk valence band. The

corresponding σ^* antibonding resonance lies in the bulk conduction band, starting at +3 eV above E_F at K, dipping to 2.8 eV as Γ is approached, rising to 3.5 eV at Γ, and continuing to 8 eV at M. No surface-derived features are seen in the bulk energy gap, consistent with the normalized conductivity data plotted in Fig. 1(c). We note that the bombardment process produces many electrons with nonzero $k_{\parallel}$; we are not restricted to vertical processes for this experiment. The optimum kinetic energy for the σ-σ^* transition is then calculated as $\sim$6 eV, in excellent agreement with the data in Fig. 3. These calculations are also supported by early-electron-loss data of Ibach and Rowe,[14] which show an optical transition centered around 8.5 eV. We point out that the Si-H bonding orbital band is extremely broad throughout most of the zone, which is reflected in the FWHM in the data. Essentially we are promoting electrons from the bulk valence band to the better defined Si-H antibonding band, breaking the Si-H bond, and in a small number of cases desorbing the atomic hydrogen from the surface before the bond can be reformed. When a critical density of surface sites has been desorbed, the Si(111) surface lowers its free energy through a spontaneous phase transition to the 2×1 π-bonded chain, desorbing the remaining hydrogen in the converted area. Because of the π bonding, it is not likely that atomic hydrogen would be stable on a 2×1 surface; the 2×1 regions we have examined show tunneling spectra nearly identical to that obtained on the clean 2×1 surface[10,11] with neither additional or missing features.

For the single-electron Auger-like process described above, one would expect the efficiency to decrease roughly as $1/\sqrt{E}$ as the energy is increased far above resonance. This is indicated in the data in Fig. 3 for kinetic energies between 6 and 8 eV. We suspect that the upturn in the conversion efficiency above 8.5 eV is due to both the onset of the optical transition at 8.5 eV [14] and to the production of secondary electrons by the now more energetic primary electrons, translating the process back to the low-energy side of the curve. We have observed that the lateral extent of the conversion process increases quite rapidly as higher electron energies are employed, more than can be accounted for by the increased tip-sample separation, providing further evidence for this secondary-emission process.

The local, atomic-scale conversion of the H-terminated 1×1 surface to the 2×1 π-chain surface provides convincing evidence for the existence of a low-activation-barrier path between the 1×1 dangling-bond surface and the 2×1 π-bonded chain surface as postulated by Northrup and Cohen[15] and confirmed in a recent *ab initio* molecular-dynamics study.[16] Even more important, we may now, with the STM, follow the electron-stimulated desorption (ESD) of a majority species without interference from reactions occurring at defects and steps, in contrast to area-averaging ESD experiments.

In summary, we have examined the surface of a Si(111):H-1×1 sample as prepared by wet HF chemical methods with no further surface treatment under UHV conditions. The surfaces are relatively clean, with clearly visible step risers and flat terraces. High-resolution images show the terraces as 1×1 with electronic characteristics consistent with the bulk structure of Si. We have demonstrated that the atomic hydrogen terminating the surface may be selectively removed by low-energy electron bombardment from the STM tip, with the resultant surface spontaneously converting to the 2×1 π-bonded chain. Measurements of the efficiency of this process as a function of electron energy demonstrate that the mechanism is one of promoting an electron from the Si-H σ to the σ^* band, desorbing the terminating hydrogen, and rendering the 1×1 surface energetically unstable with respect to the 2×1.

[1]R. C. Henderson, J. Electrochem. Soc. **119**, 772 (1972).

[2]R. D. Bringans, R. I. G. Uhrberg, R. Z. Bachrach, and J. E. Northrup, Phys. Rev. Lett. **55**, 533 (1985); J. R. Patel, J. A. Golovchenko, P. E. Freeland, and H-J. Gossmann, Phys. Rev. B **36**, 7715 (1987); R. S. Becker, B. S. Swartzentruber, J. S. Vickers, M. S. Hybertsen, and S. G. Louie, Phys. Rev. Lett. **60**, 116 (1988); R. S. Becker, T. Klitsner, and J. S. Vickers, J. Microsc. **152**, 157 (1988).

[3]Y. J. Chabal, Surf. Sci. **168**, 594 (1986); Y. J. Chabal, G. S. Higashi, and S. B. Christman, Phys. Rev. B **28**, 4472 (1983).

[4]G. S. Higashi, Y. J. Chabal, G. W. Trucks, and K. Raghavachari, Appl. Phys. Lett. **56**, 656 (1990).

[5]P. Dumas, Y. J. Chabal, and G. S. Higashi, Phys. Rev. Lett. **65**, 1124 (1990).

[6]R. S. Becker, B. S. Swartzentruber, J. S. Vickers, and T. Klitsner, Phys. Rev. B **39**, 1633 (1989).

[7]We have varied the load-locking conditions over a wide range, with the contamination shown in Fig. 1 representing a minimum. We suspect the adsorbed material is hydrocarbons from either the load-lock pumping, or the same cracked by the ion-pump discharge during transfer. A further possibility is NH_3 not removed during final rinsing, but this is considered less likely due to the results obtained in Ref. 4.

[8]J. A. Appelbaum and D. R. Hamann, Phys. Rev. Lett. **34**, 806 (1975).

[9]R. S. Becker, T. Klitsner, and J. S. Vickers, Phys. Rev. B **38**, 3539 (1988).

[10]J. A. Stroscio, R. M. Feenstra, and A. P. Fein, Phys. Rev. Lett. **57**, 2579 (1986).

[11]R. M. Feenstra, J. A. Stroscio, and A. P. Fein, Surf. Sci. **181**, 295 (1987).

[12]R. S. Becker, J. A. Golovchenko, and B. S. Swartzentruber, Phys. Rev. Lett. **55**, 987 (1985).

[13]M. Schluter and M. L. Cohen, Phys. Rev. B **17**, 716 (1978).

[14]H. Ibach and J. E. Rowe, Surf. Sci. **43**, 481 (1974).

[15]J. E. Northrup and M. L. Cohen, Phys. Rev. Lett. **49**, 1349 (1982).

[16]F. Ancilotto, W. Andreoni, A. Selloni, R. Car, and M. Parrinello, IBM Research Report No. RZ-1996(70617), 1990 (unpublished).

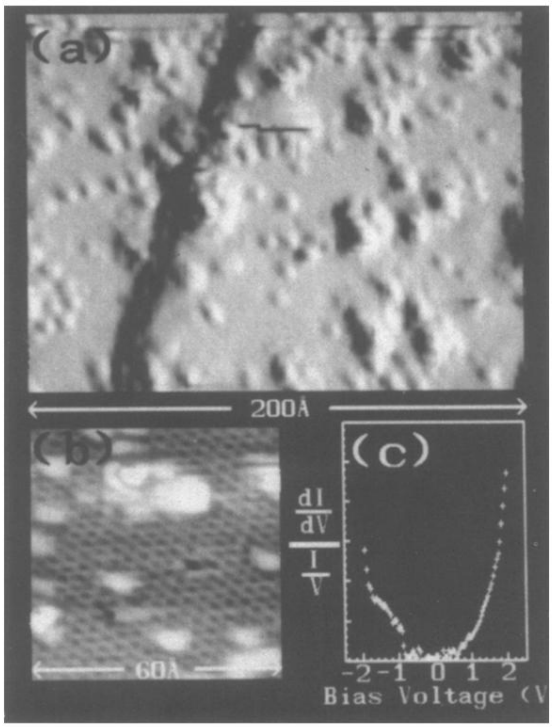

FIG. 1. (a) Tunneling image of the *as-prepared* Si(111):H-1×1 surface. (b) High-resolution image of the same showing details of the 1×1 structure. Tunneling spectrum for the 1×1 surface plotted as $(dI/dV)/(I/V)$ vs applied bias, with positive values denoting tunneling from the tip to the unoccupied sample states. The images in (a) and (b) were taken at +2.0 V at 250 pA demanded tunneling current, tunneling from the tip into empty sample states.

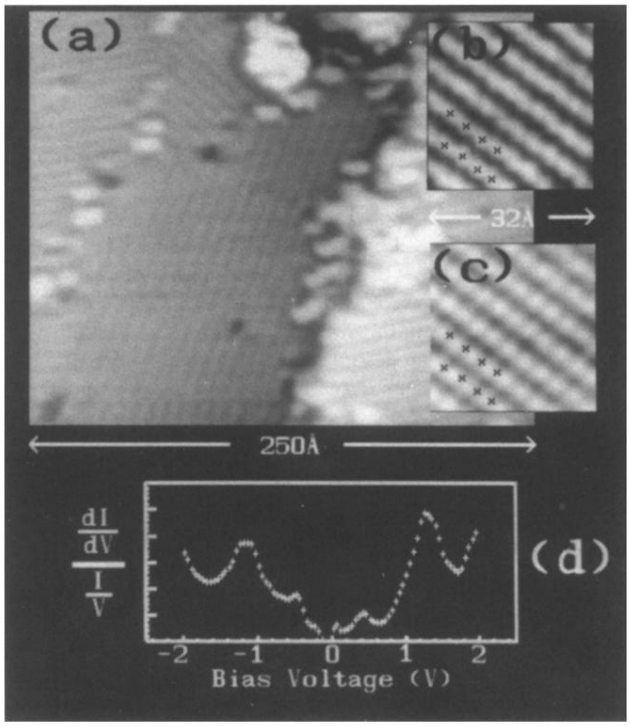

FIG. 2. (a) Tunneling images of the electron-bombarded 1×1 surface showing the resulting 2×1 domains. Simultaneous high-resolution images of one 2×1 domain depicting the phase shift along $\langle\bar{1}10\rangle$ between (b) unoccupied states and (c) occupied states. Tunneling spectrum for the 2×1 surface plotted as $(dI/dV)/(I/V)$ vs applied bias in the same manner as Fig. 1(c). The image in (a) was taken at $+1.5$ V at 1 nA demanded tunneling current, while the images in (b) and (c) were taken at $+0.8$ and -0.8 V, respectively, at 1 nA demanded tunneling current.